

Absorption Line Survey of H_3^+ toward the Galactic Center Sources III. Extent of the Warm and Diffuse Clouds*

Miwa GOTO,¹ Tomonori USUDA,² Thomas R. GEBALLE,³ Nick INDRIOLO,⁴ Benjamin J. MCCALL,⁴ Thomas HENNING,¹ and Takeshi OKA⁵

¹*Max-Planck-Institut für Astronomie, Königstuhl 17, D-69117 Heidelberg, Germany.
mgoto@mpia.de*

²*Subaru Telescope, 650, North A'ohoku Place, Hilo, HI 96720, USA.*

³*Gemini Observatory, 670, North A'ohoku Place, Hilo, HI 96720, USA.*

⁴*Department of Astronomy and Department of Chemistry, University of Illinois at Urbana-Champaign, Urbana, IL 61801-3792, USA.*

⁵*Department of Astronomy and Astrophysics, Department of Chemistry, and Enrico Fermi Institute, University of Chicago, Chicago, IL 60637, USA.*

(Received 2010 December 22; accepted 2011 February 8)

Abstract

We present follow-up observations to those of Geballe & Oka (2010), who found high column densities of H_3^+ ~ 100 pc off of the Galactic center (GC) on the lines of sight to 2MASS J17432173-2951430 (J1743) and 2MASS J17470898-2829561 (J1747). The wavelength coverages on these sightlines have been extended in order to observe two key transitions of H_3^+ , $R(3,3)^l$ and $R(2,2)^l$, that constrain the temperatures and densities of the environments. The profiles of the H_3^+ $R(3,3)^l$ line, which is due only to gas in the GC, closely matches the differences between the H_3^+ $R(1,1)^l$ and CO line profiles, just as it does for previously studied sightlines in the GC. Absorption in the $R(2,2)^l$ line of H_3^+ is present in J1747 at velocities between -60 and $+100$ km s⁻¹. This is the second clear detection of this line in the interstellar medium after GCIRS 3 in the Central Cluster. The temperature of the absorbing gas in this velocity range is 350 K, significantly warmer than in the diffuse clouds in other parts of the Central Molecular Zone. This indicates that the absorbing gas is local to Sgr B molecular cloud complex. The warm and diffuse gas revealed by Oka et al. (2005) apparently extends to ~ 100 pc, but there is a hint that its temperature is somewhat lower in the line of sight to J1743 than elsewhere in the GC. The observation of H_3^+ toward J1747 is compared with the recent Herschel observation of H_2O^+ toward Sgr B2 and their chemical relationship and remarkably similar velocity profiles are discussed.

Key words: ISM: clouds — ISM: lines and bands — ISM: molecules — Galaxy: center

1. Introduction

The study of the interstellar medium in the Galactic center using H_3^+ as an astrophysical probe was initiated by Geballe et al. (1999), who discovered that the Galactic center is the richest reservoir of H_3^+ in the Milky Way. The column density of H_3^+ toward the Galactic center is $> 10^{15}$ cm⁻², an order of magnitude higher than in dense molecular clouds (McCall et al. 1999) and in diffuse clouds in the Galactic disk (McCall et al. 2002; Indriolo et al. 2007). Studies of H_3^+ in the interstellar medium initially relied on the vibration-rotation transitions from the two lowest rotational levels, $(J, K)=(1,1)$ and $(1,0)$. The first interstellar H_3^+ line from a higher rotational level was discovered by Goto et al. (2002) toward the bright infrared sources GCIRS 3 and GCS 3-2, near the Galactic center. The $(J, K) = (3,3)$ level from which the observed $R(3,3)^l$ originates is 361 K above the lowest level, and is “metastable”, that is, H_3^+ in this level does not decay by spontaneous emission (Pan & Oka 1986).

Oka et al. (2005) determined the physical state of the gas toward the bright star GCS 3-2 in the Galactic center based on a steady state calculation of thermalization by Oka & Epp (2004). Their results are summarized as follows: (1) compared to diffuse clouds in the Galactic disk, the gas in the Galactic center producing absorption by H_3^+ has a similar density (≤ 100 cm⁻³), but a much higher temperature (~ 250 K); (2) The path length of the absorbing cloud is at least 30 pc, which means it occupies a significant portion of the volume of the Galactic center; (3) the cosmic ray ionization rate of H_2 must be at least 10^{-15} s⁻¹, with the limiting value in effect if the absorbing clouds’ line of sight dimension is the full diameter of the Central Molecular Zone of the Galaxy (CMZ) (Morris & Serabyn 1996, 200 pc).

Subsequently Goto et al. (2008) found that the interpretation by Oka et al. (2005) is universal for sightlines toward 8 stars located in the Galactic center and extending from Sgr A* to 30 pc east of Sgr A*. Without exception all eight sightlines they observed show strong $R(1,1)^l$ and $R(3,3)^l$ absorptions with similar column densities of H_3^+ as toward GCS 3-2, demonstrating that the warm and

* Based on data collected at Subaru Telescope, which is operated by the National Astronomical Observatory of Japan.

diffuse gas is present over a wide region of the CMZ.

In order to explore a wider region of the CMZ, Geballe & Oka (2010) have undertaken a spectroscopic search, from 170 pc east to 170 pc west of Sgr A*, for bright infrared stars in *Spitzer* GLIMPSE catalogue (Ramírez et al. 2008) with clean infrared continua, that can serve as background sources for H_3^+ spectroscopy. They have reported strong H_3^+ $R(1,1)^l$ and CO $v=2-0$ absorption toward two stars thus selected, 2MASS J17432173-2951430 and 2MASS J17470898-2829561 (hereafter J1743 and J1747), located 130 pc to the West and 80 pc to the East of Sgr A*, respectively. Their results strongly imply that the warm and diffuse environment revealed by Oka et al. (2005) extends to radii of ~ 100 pc.

In the present study we have observed the key $R(3,3)^l$ and $R(2,2)^l$ absorptions toward J1743 and J1747 in order to better determine the properties of these two new sightlines. The distance to the Galactic center is assumed to be 7.6 kpc throughout this paper (Eisenhauer et al. 2005; Nishiyama et al. 2006).

2. Observation and Data Reduction

Spectra of J1743 and J1747 were obtained at the Subaru Telescope on UT 4 May 2010 by the high-resolution infrared spectrograph IRCS (Kobayashi et al. 2000). The resolving power used was $R=20,000$. The angle settings of the echelle and cross-dispersing gratings were -9000 and 2400 , respectively, in order to cover H_3^+ $R(4,4)^l$ [$3.4548 \mu\text{m}$], $R(2,2)^l$ [$3.6205 \mu\text{m}$], $R(1,0)$ [$3.6685 \mu\text{m}$], and $R(1,1)^u$ [$3.6681 \mu\text{m}$], and -200 and 4000 , respectively, to cover $R(3,3)^l$ [$3.5337 \mu\text{m}$]. The data were obtained while nodding the telescope along the slit, whose dimensions were $0''.14 \times 6''.7$, so as to be able to easily subtract the thermal sky background. The positions of the targets were continuously manually centered during the observation to maximize the throughput. The centering was performed with the camera of IRCS observing the L' band, the same wavelength as the spectroscopic observation, to minimize differential atmospheric refraction. An early-type spectroscopic standard star, HR 6378 (A2 V, $V=2.43$), was observed immediately before or after the object observation through similar airmass. Standard calibration data were obtained in the morning; these included spectroscopic flat-fields with the same grating settings. The sky was clear and stable during the night, with the seeing measured as $0''.59$ in the K band. The journal of observations is shown in Table 1.

Data reduction was performed as described by Goto et al. (2008). The raw spectrograms were pair-subtracted, flat-fielded, and corrected for outlier pixels. One dimensional spectra of each of the Galactic center objects and of the standard star were extracted using IRAF¹ aperture extraction package. The spectra of the Galactic center sources were further processed using custom-written IDL

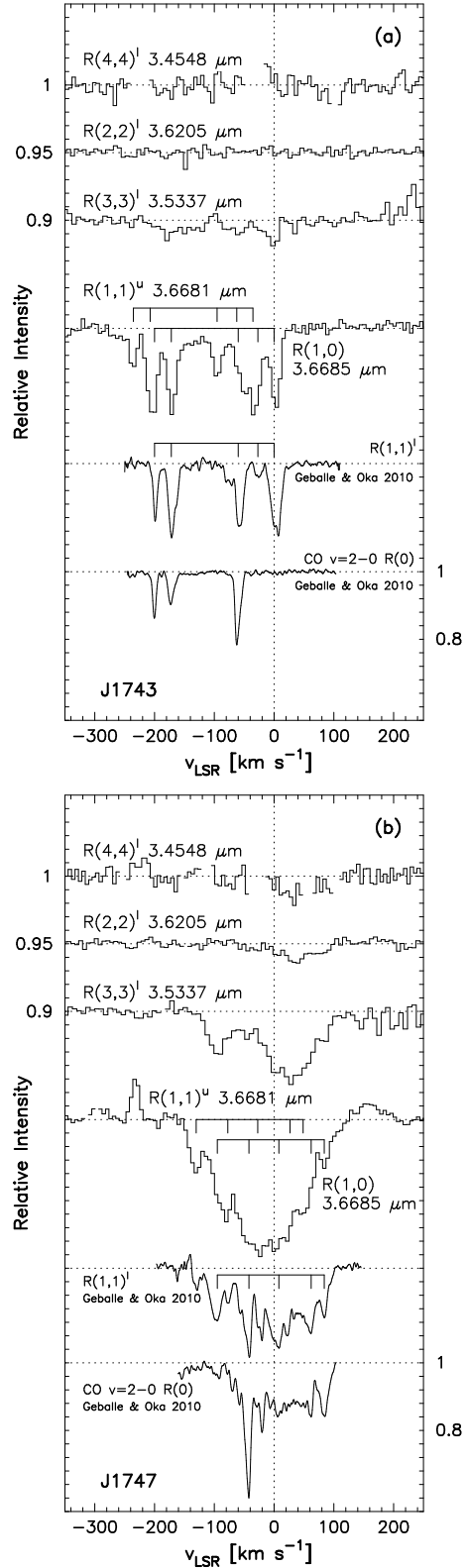


Fig. 1. Top (a): the spectra of H_3^+ at $R(4,4)^l$, $R(2,2)^l$, $R(1,0)$ [overlapped with $R(1,1)^u$] in the line of sight to 2MASS J17432173-2951430. H_3^+ $R(1,1)^l$ and CO $R(0)$ lines are taken from Geballe & Oka (2010). Bottom (b): same with the left, but for 2MASS J17470898-2829561. The velocities marked by the vertical lines are 0, -27 , -60 , -172 , and -200 km s^{-1} for J1743, and 84 , 62 , 8 , -42 , and -95 km s^{-1} for J1747.

¹ IRAF is distributed by the National Optical Astronomy Observatories, which are operated by the Association of Universities for Research in Astronomy, Inc., under cooperative agreement with the National Science Foundation.

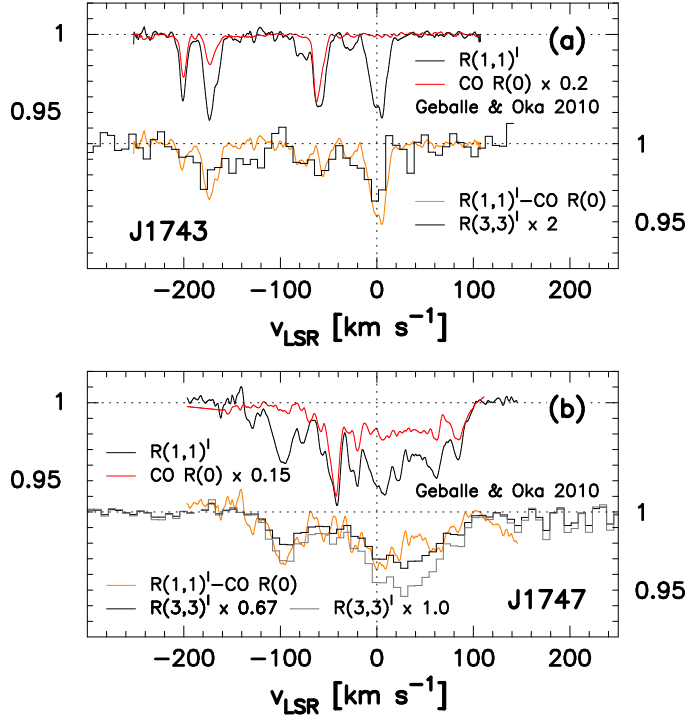


Fig. 2. Top (a): $R(1,1)^l$ and CO $R(0)$ spectra of 2MASS J17432173-2951430 taken from Geballe & Oka (2010). CO $R(0)$ is scaled by the factor of 0.2 so that the sharp absorption lines at -60 km s^{-1} are roughly with the same depth. The difference of the two spectra is shown in orange in the lower trace to compare it with $R(3,3)^l$ spectrum obtained in this study. $R(3,3)^l$ spectrum is scaled by 2 to match the differential spectra of $R(1,1)^l$ and CO $R(0)$. Bottom (b): same as the top, but for 2MASS J17470898-2829561. CO $R(0)$ is scaled by 0.15 so that the absorption line at -42 km s^{-1} is roughly the same depth with $R(1,1)^l$. The differential spectrum of $R(1,1)^l$ and CO $R(0)$ is compared in the lower trace. $R(3,3)^l$ matches well with the differential spectrum at $> -60 \text{ km s}^{-1}$ after scaling by 0.67 (black trace), while the scaling factor is close to unity at $< -60 \text{ km s}^{-1}$ (gray trace).

codes for correction for the telluric absorption lines, using the spectra of the standard star. Slight wavelength offsets, differences in airmass, fringes on the continuum, and saw-tooth features produced by different readout channels were simultaneously removed. Wavelength calibration was performed by maximizing the correlation with a model atmospheric transmission curve calculated using ATRAN (Lord 1992) and is better than 1 km s^{-1} . Wavelengths were converted to radial velocities with respect to the local standard of the rest, using IRAF *rv* package. Normalized absorption spectra of H_3^+ are shown in Fig. 1 for J1743 and J1747, together with the H_3^+ and CO spectra from Geballe & Oka (2010).

3. Results

The spectra of H_3^+ $R(1,1)^l$ and the CO $v=2-0$ $R(0)$ line in Geballe & Oka (2010) are considerably different from each other. Here we compare in detail the difference spec-

tra of those two lines to the $R(3,3)^l$ line profiles observed here.

The upper traces of Fig. 2a superimpose the velocity profiles of the H_3^+ $R(1,1)^l$ and CO $R(0)$ lines in J1743 taken from Geballe & Oka (2010), but after rescaling CO $R(0)$ by a factor of 0.2 so that the common absorption components at -60 km s^{-1} , which probably both arise solely in dense molecular gas in the foreground 3 kpc spiral arm as discussed by e.g., Oka et al. (2005), are roughly the same depth. In J1743 the H_3^+ $R(1,1)^l$ line profile consists of six distinct absorptions, at 0, -27 , -60 , -75 , -172 , -200 km s^{-1} , with minor substructure in the -172 and 0 km s^{-1} components (Geballe & Oka 2010). The CO $v=2-0$ line shows only three of these features: at -60 , -172 and -200 km s^{-1} . Perhaps most remarkably the CO profile is completely lacking the 0 km s^{-1} component, which is the strongest component in the H_3^+ $R(1,1)^l$ profile. The lower trace in orange represents the difference spectrum of $R(1,1)^l$ and the scaled CO $R(0)$ overlaid with $R(3,3)^l$ from the present study. Despite being at lower spectral resolution than Geballe & Oka (2010), the $R(3,3)^l$ profile qualitatively reproduces the difference spectrum, showing absorption components at 0, -75 km s^{-1} as well as the extra absorption at -172 km s^{-1} . The two cloud components with the high negative velocities of -200 km s^{-1} and -172 km s^{-1} are due to local dense clouds in Sgr E as previously observed by Liszt (1992).

The spectra of J1747 follow the same pattern. The upper traces of Fig. 2b are the H_3^+ $R(1,1)^l$ and CO $2-0$ $R(1)$ lines in J1747 (Geballe & Oka 2010), after rescaling the CO line by a factor of 0.15, so that the common absorption components at -42 km s^{-1} , which probably arise in dense cloud material in the foreground 3 kpc spiral arm, are the same depth. The absorption by CO $v=2-0$ at negative velocities cuts off at -60 km s^{-1} , unlike the absorption by H_3^+ $R(1,1)^l$, which extends to -150 km s^{-1} . The absorptions by H_3^+ $R(1,1)^l$ and CO have similar extents at positive velocities but that of H_3^+ is much stronger than CO $v=2-0$ after scaling. Again the $R(3,3)^l$ profile reproduces the extra absorption of $R(1,1)^l$ well, with two broad absorption components, from -120 to -60 km s^{-1} and from -60 to 100 km s^{-1} . The rule that CO and H_3^+ $R(3,3)^l$ separately trace dense and diffuse gas in a line of sight, respectively, while $R(1,1)^l$ traces both of them (Oka et al. 2005), thus also applies to J1743 and J1747. This consistency lends support to the idea that the warm and diffuse clouds found on sightlines within 30 pc of the Galactic nucleus are present out to $\sim 100 \text{ pc}$.

Closer examination of the J1747 data reveals that the scaling factors of $R(3,3)^l$ needed to match $R(1,1)^l$ are slightly different at $< -60 \text{ km s}^{-1}$ and $> -60 \text{ km s}^{-1}$. The $R(1,1)^l - \text{CO } R(0)$ difference spectrum matches the $R(3,3)^l$ at $> -60 \text{ km s}^{-1}$ when scaling $R(3,3)^l$ by 0.67 (black trace in Fig. 2b), while the scaling factor at $< -60 \text{ km s}^{-1}$ is close to unity (gray trace). This is most simply interpreted as a temperature effect. The $> -60 \text{ km s}^{-1}$ absorption is probably local to the Sgr B star forming region (Geballe & Oka 2010), as is seen in the broad and strong absorption of CO $v=2-0$. We infer

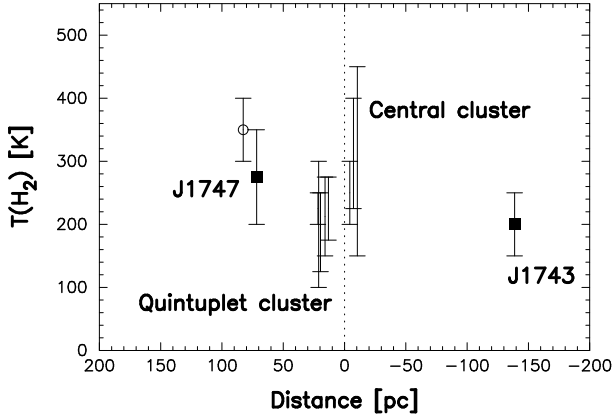


Fig. 3. Temperature distribution in the CMZ as a function of the distance from the Galactic nucleus. The distance to the Galactic center is assumed to be 7.6 kpc. The data for the Central cluster and the Quintuplet cluster are taken from Goto et al. (2008). The open circle is for the positive velocity component in 2MASS J17470898-2829561, which is likely locally associated to Sgr B star forming region.

that the absorbing gas in Sgr B is warmer and thus produces a higher $n(3,3)/n(1,1)$ ratio. The $< -60 \text{ km s}^{-1}$ absorption probably arises in the somewhat cooler diffuse clouds elsewhere in the CMZ.

The equivalent widths of the absorption lines in the warm and diffuse gas have been converted to the column densities in the $v=0$ (1,1), (2,2) and (3,3) levels in the same manner as Geballe et al. (1999); Goto et al. (2002). The squares of transition dipole moments used for $R(1,1)^l$, $R(2,2)^l$, $R(3,3)^l$, and $R(4,4)^l$, 0.0141, 0.0177, 0.0191, and 0.0198 D^2 , respectively, are based on the Einstein A coefficients given in Neale, Miller, & Tennyson (1996). The densities and the temperatures of the absorbing clouds were determined from the relative populations of H_3^+ in $(J,K)=(1,1)$, (2,2) and (3,3), using the steady state model of Oka & Epp (2004). The detection of the $R(2,2)^l$ line toward J1747, only the second detection of this line, allows the density in this sightline to be determined, rather than an upper limit. The results are shown in Table 2. Fig. 3 shows the temperature distribution in the CMZ as a function of the distance from the Galactic nucleus. The cloud temperatures observed so far in the CMZ are in the range 100–400 K. There is some possibility that temperatures are lower in the line of sight to J1743 than elsewhere.

4. Discussion

The region containing warm and diffuse gas is now 7 times more extensive in Galactic longitude than originally found by Goto et al. (2008). This environment remains exclusive to the CMZ of the Galactic center, as $R(3,3)^l$ has not been detected in the clouds in the Galactic disk. How far beyond a radius of 100 pc the outer boundary of the cloud is yet to be determined. Although the observations reported in this paper are only toward two stars, one 130 pc West and the other 80 pc East, additional ob-

servations toward several other stars between them (Oka et al., in preparation) yield comparable column densities of H_3^+ in warm and low density clouds, further suggesting that this environment exists throughout the CMZ with a large volume filling factor.

The recent detections of strong far infrared absorption by H_2O^+ toward Sgr B2 (Schilke et al. 2010) using the HIFI instrument on the Herschel Space Observatory have given independent evidence for the existence of a large amount of diffuse gas in the CMZ. Because H_2O^+ is produced from OH^+ through the hydrogen abstraction reaction $OH^+ + H_2 \rightarrow H_2O^+ + H$, and OH^+ is produced either from O^+ by the hydrogen abstraction reaction $O^+ + H_2 \rightarrow OH^+ + H$, or from O by the proton hop reaction $O + H_3^+ \rightarrow OH^+ + H_2$, H_2O^+ is closely related chemically to H_3^+ . H_2O^+ is rapidly destroyed by H_2 through hydrogen abstraction reaction $H_2O^+ + H_2 \rightarrow H_3O^+ + H$, so it cannot be abundant in dense clouds. Gerin et al. (2010) and Neufeld et al. (2010) who observed strong absorption by both OH^+ and H_2O^+ toward W31C and W49N, respectively, have concluded from chemical analysis that these molecular ions are found in diffuse gas with a very low fraction of molecular hydrogen, $f(H_2)$. Unlike H_3^+ they cannot be used to determine temperatures directly because due to their large dipole moments, only the lowest levels are populated. The “spin” temperature determined from the observed ortho to para ratio of H_2O^+ is not straightforward to interpret in terms of a kinetic temperature. Gerin et al. (2010) estimate $T \sim 100$ K.

In addition to the chemical connection between H_2O^+ and H_3^+ , there is some direct observational evidence that the two species are co-located. The velocity profiles of ortho- and para- H_2O^+ reported by Schilke et al. (2010) (see their Figs. 1 and 2) are remarkably similar to the H_3^+ velocity profile toward J1747 of Geballe & Oka (2010) reproduced in Figs. 1 and 2 of this paper. Not only do both range from $\sim -120 \text{ km s}^{-1}$ to $\sim 90 \text{ km s}^{-1}$, but also the velocities of individual peaks approximately match. The identical peaks at -48 km s^{-1} , -26 km s^{-1} , and 4 km s^{-1} , which are due to the three foreground spiral arms, are not surprising. However, the absorption peaks near -100 km s^{-1} and 60 km s^{-1} , which are due to gas within the GC, also match (Oka 2010). Similar agreement is observed between the velocity profiles of $^{13}CH^+$ (E. Falgarone, private communication) and H_3^+ . We regard these as strong indications that H_2O^+ , CH^+ and H_3^+ are largely found together. This is somewhat surprising since H_2O^+ and CH^+ require low $f(H_2)$ while H_3^+ favors high $f(H_2)$. The locations of Sgr B2 and J1747 are separated in the plane of the sky by 16 pc. The velocity correspondence may be due to the large extents of diffuse clouds within the Sgr B complex.

We thank the staff of the Subaru Telescope and NAOJ for invaluable assistance in obtaining these data. This research has made use of the SIMBAD database, operated at CDS, Strasbourg, France. We also thank the referee, J.H. Black, for suggesting that we discuss relevant results from the Herschel Observation. T.R.G.’s research is sup-

ported by the Gemini Observatory, which is operated by the Association of Universities for Research in Astronomy, Inc., on behalf of the international Gemini partnership of Argentina, Australia, Brazil, Canada, Chile, the United Kingdom and the United States of America. B.J.M. and N.I. have been supported by NSF Grant PHY 08-55633. T.O. acknowledges NSF Grant AST 08-49577. We appreciate the hospitality of the local Hawaiian community that made possible the research presented here.

References

- Eisenhauer, F., Genzel, R., Alexander, T., Abuter, R., Paumard, T., Ott, T., Gilbert, A., Gillessen, S., Horrobin, M., Trippe, S., Bonnet, H., Dumas, C., Hubin, N., Kaufer, A., Kissler-Patig, M., Monnet, G., Ströbele, S., Szeifert, T., Eckart, A., Schödel, R., & Zucker, S., 2005, *ApJ*, 628, 246
- Geballe, T. R. & Oka, T. 2010, *ApJL*, 709, L70
- Geballe, T. R., McCall, B. J., Hinkle, K. H., & Oka, T. 1999, *ApJ*, 510, 251
- Gerin, M. et al. 2010, *A&A*, 518, L110
- Goto, M., McCall, B. J., Geballe, T. R., Usuda, T., Kobayashi, N., Terada, H., & Oka, T. 2002, *PASJ*, 54, 951
- Goto, M., Usuda, T., Nagata, T., Geballe, T.R., McCall, B. J., Indriolo, N., Suto, H., Henning, Th., Morong, C. P., & Oka, T. 2008, *ApJ*, 688 306
- Indriolo, N., Geballe, T. R., Oka, T., & McCall, B. J. 2007, *ApJ*, 671, 1736
- Lord, S. D. 1992, A New Software Tool for Computing Earth's Atmosphere Transmissions of Near- and Far-Infrared Radiation, NASA Technical Memoir 103957 (Moffett Field, CA: NASA Ames Research Center)
- Kobayashi, N., Tokunaga, A. T., Terada, H., Goto, M., Weber, M., Potter, R., Onaka, P. M., Ching, G. R., et al. 2000, *Proc. SPIE*, 4008, 1056
- Liszt, H. S. 1992, *ApJS*, 82, 425
- McCall, B. J., Geballe, T. R., Hinkle, K. H., & Oka, T. 1999, *ApJ*, 522, 338
- McCall, B. J., Hinkle, K. H., Geballe, T. R., Moriarty-Schieven, G. H., Evans, N. J., II, Kawaguchi, K., Takano, S., Smith, V. V., & Oka, T. 2002, *ApJ*, 567, 391
- Morris, M., & Serabyn, E. 1996, *ARA&A*, 34, 645
- Neale, L, Miller, S., & Tennyson, J. 1996, *ApJ*, 464, 516
- Neufeld, D.A. et al. 2010, *A&A*, 521, L26
- Nishiyama, S., Nagata, T., Sato, S., Kato, D., Nagayama, T., Kusakabe, N., Matsunaga, N., Naoi, T., Sugitani, K., & Tamura, M. 2006, *ApJ*, 647, 1093
- Oka, T., & Epp, E. 2004, *ApJ*, 613, 349
- Oka, T., Geballe, T. R., Goto, M., Usuda, T., & McCall, B. J. 2005, *ApJ*, 632, 882
- Oka, T., in the Proceedings of Symposium, Spectroscopy of Molecular Ions in the Laboratory and in Space, AIP Conference Proceedings in press. Available at <http://Fermi.uchicago.edu/~smiles>.
- Pan, F.-S., & Oka, T. 1986, *ApJ*, 305, 518
- Ramírez, S. V., Arendt, R. G., Sellgren, K., Stolovy, S. R., Cotera, A., Smith, H. A., & Yusef-Zadeh, F. 2008, *ApJS*, 175, 147
- Schilke, P. et al. 2010, *A&A*, 521, L11

Table 1. Journal of observations.

| | l | b | L | Lines covered | Exposure [s] | Grating* | | Standard | |
|------------------------------|----------------|----------------|-----|--|-----------------|----------|------|----------|------|
| | [$^{\circ}$] | [$^{\circ}$] | | | | ECH | XDP | Name | Spe. |
| 2MASS J17432173-2951430. ... | -1.046 | -0.065 | 3.8 | $R(4,4)^l, R(2,2)^l, R(1,1)^u, R(1,0)$ | 960 | -9000 | 2400 | HR 6378 | A2 V |
| | | | | $R(3,3)^l$ | 480 | -200 | 4000 | HR 6378 | A2 V |
| 2MASS J17470898-2829561. ... | 0.548 | -0.059 | | $R(4,4)^l, R(2,2)^l, R(1,1)^u, R(1,0)$ | 5400 | -9000 | 2400 | HR 6378 | A2 V |
| | | | | $R(3,3)^l$ | 5400 | -200 | 4000 | HR 6378 | A2 V |

* “ECH” and “XDP” denote the motor settings for the angles of echelle and cross-dispersing gratings in the instrumental unit.

Table 2. Column densities of H_3^+ toward 2MASS 1747 and 2MASS 1743.

| | Δv^a [km s^{-1}] | $N(1,1)$ [10^{14}cm^{-2}] | $N(3,3)$ [10^{14}cm^{-2}] | $N(2,2)^d$ [10^{14}cm^{-2}] | $N(4,4)^d$ [10^{14}cm^{-2}] | $n(3,3)/n(1,1)$ | $n(3,3)/n(2,2)$ | $n(\text{H}_2)$ [cm^{-3}] | $T(\text{H}_2)$ [K] |
|------------------------------|--|--|--|--|--|-----------------|-----------------|---|------------------------|
| 2MASS J17470898-2829561. ... | -150, -60 ^b | 6.0 ± 0.7 | 4.3 ± 1.3 | < 0.8 | < 1.8 | 0.7 ± 0.2 | > 5.4 | < 50 | 200–350 |
| | -60, +100 ^c | 16.4 ± 1.2 | 18.2 ± 2.2 | 5.8 ± 1.5 | < 3.3 | 1.1 ± 0.2 | 3.1 ± 0.9 | 100–150 | 300–400 |
| 2MASS J17432173-2951430. ... | -220, +20 | 12.8 ± 1.9 | 5.7 ± 2.2 | < 2.1 | < 5.0 | 0.45 ± 0.2 | > 2.9 | < 50 | 150–250 |

^a The interval that the column densities are calculated. ^b The CMZ component. ^c Sgr B component. ^d The upper limits are for 1σ .